Supplementary Materials
Molecular Biology of the Cell
Knöringer *et al*.

Supplementary Figures

Supplementary Figure 1. GO Enrichment Analysis of late changes in the proteome of clogger-expressing cells. (A-B) Enrichment of GO terms of the "molecular function" category of proteins upregulated (log_2 fold change larger than 0.5 with adjusted p value of at most 0.05) in cells expressing b_2-DHFR compared to cytosolic DHFR after 4.5 h (A) or 9 h (B) of induction with 0.5% galactose. Proteomics data from (Boos *et al.*, 2019).

Supplementary Figure 2. Detection of UPR^{ER} induction with mass spectrometry and RT-qPCR. (A) Protein levels in clogger-expressing versus control cells after different times of induction were measured by quantitative mass spectrometry (Boos *et al.*, 2019). Highlighted are proteins which are reported UPR^{ER} targets (Schmidt *et al.*, 2019). Data from *n*=3 independent biological replicates are shown. The data for 18 h are the same as shown in Figure 1E. **(B)** The change in translational efficiency after 4.5 h clogger expression was calculated for all genes measured in both the RNA-seq(Boos *et al.*, 2019) and Ribo-Seq on clogger-expressing cells by dividing the translatome fold change by the transcriptome fold change. **(C)** Schematic depiction of the primer-probe combinations used to quantify total *HAC1* as well as spliced *HAC1*^{i} mRNA levels via RT-qPCR. **(D)** Wild type, Δ*ire1* and Δ*hac1* cells were grown in presence or absence of 1 µg/ml tunicamycin and *HAC1* and *HAC1*^{i} levels were analyzed with the primer-probe assay shown in C. As expected, *HAC1*^{i} levels increased in wild type cells treated with tunicamycin, but no *HAC1*^{i} was detected in cells lacking *HAC1* or *IRE1*, confirming the specificity of the RT-qPCR assay.

Supplementary Figure 3. Clogger-induced growth defects are not due to elevated cell death. (A-B) Cell viability of wild type, Δ*ire1* and Δ*hac1* cultures expressing either cytosolic DHFR or b2-DHFR was assessed with propidium iodide (PI) staining, subsequent flow cytometry and quantification of the fraction of PI negative cells. Cells in which no ectopic gene was expressed, that were not stained with PI or that were killed by incubation at 70°C for 30 min served as controls (A). Clogger expression does not result in cell death (B).

Supplementary Figure 4. Cytosolic peroxide levels are not elevated upon clogger expression or in UPR^{ER}-deficient cells. (A) The roGFP2-Tsa2ΔC$_R$ probe reacts with peroxides, which ultimately results in the formation of an intramolecular disulfide bond between two cysteine residues adjacent to the GFP chromophore. This changes the excitation spectrum of roGFP2, which can be measured and used as a proxy for probe oxidation (see Methods for details). (B-C) Wild type and Δ*hac1* cells that express either cytosolic or *b*$_2$-DHFR (induced for 4.5 h), as well as the roGFP2-Tsa2ΔC$_R$ (constitutively expressed) in the cytosol (B) or in mitochondria (C, Su9- roGFP2-Tsa2ΔC$_R$) were analyzed in a fluorescence plate reader. Fluorescence of roGFP2 was followed for 4 min before H_2O_2 was added at final concentration of 0, 10, 50 or 100 µM. Responses to the treatment were monitored for 1 h (B) or 1.5 h (C). Probe oxidation (OxD) was calculated from fluorescence intensities obtained by excitation at 405 nm and 490 nm (see Methods for details). (D) For the data shown in b, the 0 µM H_2O_2 baseline was subtracted from the H_2O_2-challenged samples and differences in probe oxidation after H_2O_2 addition was analyzed.

Supplementary Figure 5. Mitochondrial morphology changes precede ER localization of Oxa1. (A) The mitochondrial inner membrane protein Oxa1 was genomically tagged with ymNeonGreen, the ER marker Sec63 was tagged with ymScarletI. Confocal fluorescence microscopy was performed after 4.5 h of expression of either b_2-DHFR or cytosolic DHFR. When the clogger was induced, a fraction of Oxa1-ymNeonGreen colocalized with Sec63-ymScarletI. Scale bar, 5 µm. (B) Cells expressing Oxa1-GFP^{11} and Oxa1-GFP$^{1-10}$ and either cytosolic DHFR or b_2-DHFR were imaged at indicated times after clogger induction with a fluorescence microscope. Clogger-induced changes in mitochondrial morphology were observed 1 hour after induction (yellow arrows), ER localization after 3 hours (red arrows).

Supplementary Figure 6. A split-GFP assay to assess the subcellular localization of mitochondrial precursor proteins. (A) The GFP^{11} fragment was fused to Oxa1, Om45, Mia40 and Dld1, and the GFP^{1-10} reporter was fused to Oxa1 (mitochondrial inner membrane, matrix side), Mia40 (mitochondrial inner membrane, IMS side), Sec63 (ER membrane, cytosolic side) and Ssa1 (cytosol). (B-D) The split-GFP constructs described in panel a were co-expressed with b_2-DHFR or cytosolic DHFR and fluorescence was measured with a plate reader after 4.5 h of galactose induction. Under non-stressed conditions (expression of cytosolic DHFR), the split-GFP signals recapitulated the known localizations of Oxa1, Om45, Mia40 and Dld1. Under mitoprotein-induced stress (b_2-DHFR expression), Om45-GFP^{11} also evoked a fluorescence signal when combined with Sec63-GFP^{1-10} and Ssa1-GFP^{1-10}, indicating accumulation at the cytosolic side of the ER membrane. (E) Fluorescence microscopy of cells expressing Oxa1-GFP^{11} and Oxa1-GFP^{1-10} (left) or Oxa1-GFP^{11} and Sec63-GFP^{1-10} (right) and either b_2-DHFR or cytosolic DHFR after 4.5 h of induction. Scale bar, 5 µm. (F) WT, Δ*doa10*, Δ*hac1* and Δ*yos9* cells expressing Oxa1-GFP^{11} and Sec63-GFP^{1-10} were cultured with either 0 or 50 µM carbonyl cyanide m-chlorophenylhydrazone (CCCP) for 16 h and fluorescence was measured.

Supplementary Figure 7. Certain mitochondrial proteins are constitutively synthesized close to the ER surface. (A) Data from (Fazal *et al.*, 2019) on the subcellular distribution of mRNA in HEK293T cells. The biotin ligase APEX2 was localized to the ER or mitochondria and biotinylated mRNAs were purified and sequenced (APEX-Seq). For all mitochondrial proteins in the dataset, the $\log_2$ enrichment of mRNAs at the ER membrane (ERM-APEX2) and the mitochondrial outer membrane (OMM-APEX2) over the total mRNAs are shown. While most mRNAs localize to the mitochondrial membrane, some transcripts are also enriched near the ER surface. (B) Potential glycosylation sites in the Oxa1 sequence were predicted with the NetNGlyc 1.0 Server (Gupta and Brunak, 2002). Underlined motifs are predicted to be luminal if Oxa1 was inserted into the ER membrane (Weill *et al.*, 2019a). (C) Lysates from cells expressing *GAL*-Oxa1-HA and either cytosolic DHFR or b_2-DHFR for 4.5 hours were treated with EndoH and analyzed by Western blotting against the HA tag on Oxa1 alongside untreated lysates. The EndoH-sensitive band (asterisk) denotes a glycosylated form of Oxa1. p, unmodified precursor form of Oxa1, m, mature Oxa1. (D) Quantification of EndoH-sensitive bands from n=3 Western Blots against Oxa1-HA in cells expressing either cytosolic DHFR or b_2-DHFR. The fraction of glycosylated Oxa1 increases with clogger expression, but is already present under physiological conditions.

Supplementary Figure 8. The UPR^{ER} is required for efficient growth upon metabolic switches and mitoprotein-induced stress. (A) Maximum growth rate *r* of the cultures shown in Figure 5B. (B-C) Maximum capacity *k* and maximum growth rate *r* of the cultures shown in Figure 5E. *p* values for pairwise comparisons with a significant difference ($p < 0.05$) are shown. (D) Schematic depiction of the LexA-ER expression system used to express *HAC1*^{i} independently of the clogger. Upon binding of β-estradiol to the estrogen receptor domain, the transcription factor LexA-ER-AD binds to lexO elements upstream of the *HAC1*^{i} ORF and stimulates its transcription. (E) Wild type cells and cells that express *HAC1*^{i} from a lexO promoter driven by the β-estradiol-inducible artificial transcription factor LexA-ER-AD were grown to log phase in lactate medium. Clogger expression was induced by addition of 0.5% galactose and at the same time, the media were supplemented with the indicated concentration of β-estradiol. Ectopic expression of low levels of *HAC1*^{i} did not result in better growth of clogger-expressing cells. (F) Maximum growth rate *r* of the cultures shown in Panel E.

Supplementary Tables

Supplementary Table 1. Yeast strains used in this study.

Supplementary Table 2. Plasmids used in this study.

Supplementary Table 3. Primers used in this study.

Supplementary Table 4. Numerical source data for all experiments.

Supplementary Table 5. Ribosome profiling data.

A

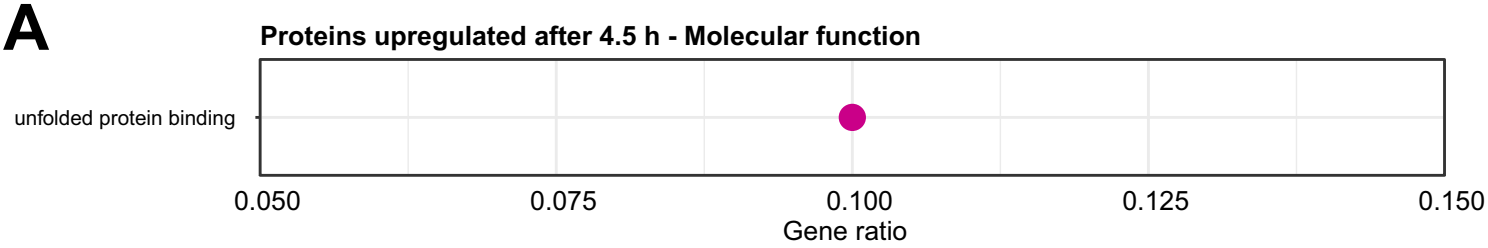
Proteins upregulated after 4.5 h - Molecular function
unfolded protein binding
0.050
0.075
0.100
0.125
0.150
Gene ratio

B

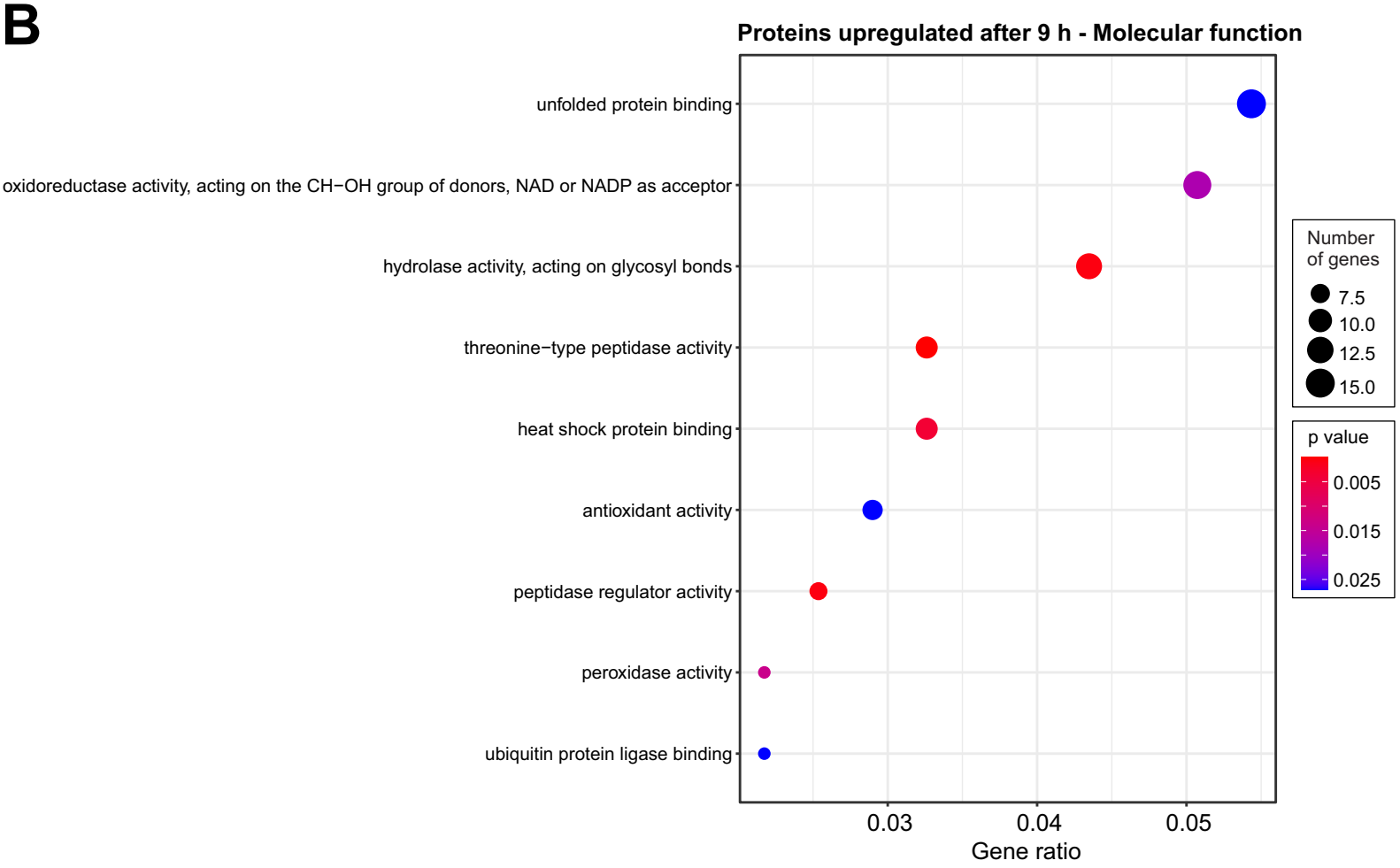
Proteins upregulated after 9 h - Molecular function
unfolded protein binding
oxidoreductase activity, acting on the CH−OH group of donors, NAD or NADP as acceptor
hydrolase activity, acting on glycosyl bonds
threonine−type peptidase activity
heat shock protein binding
antioxidant activity
peptidase regulator activity
peroxidase activity
ubiquitin protein ligase binding
0.03
0.04
0.05
Gene ratio
Number of genes
7.5
10.0
12.5
15.0
p value
0.005
0.015
0.025

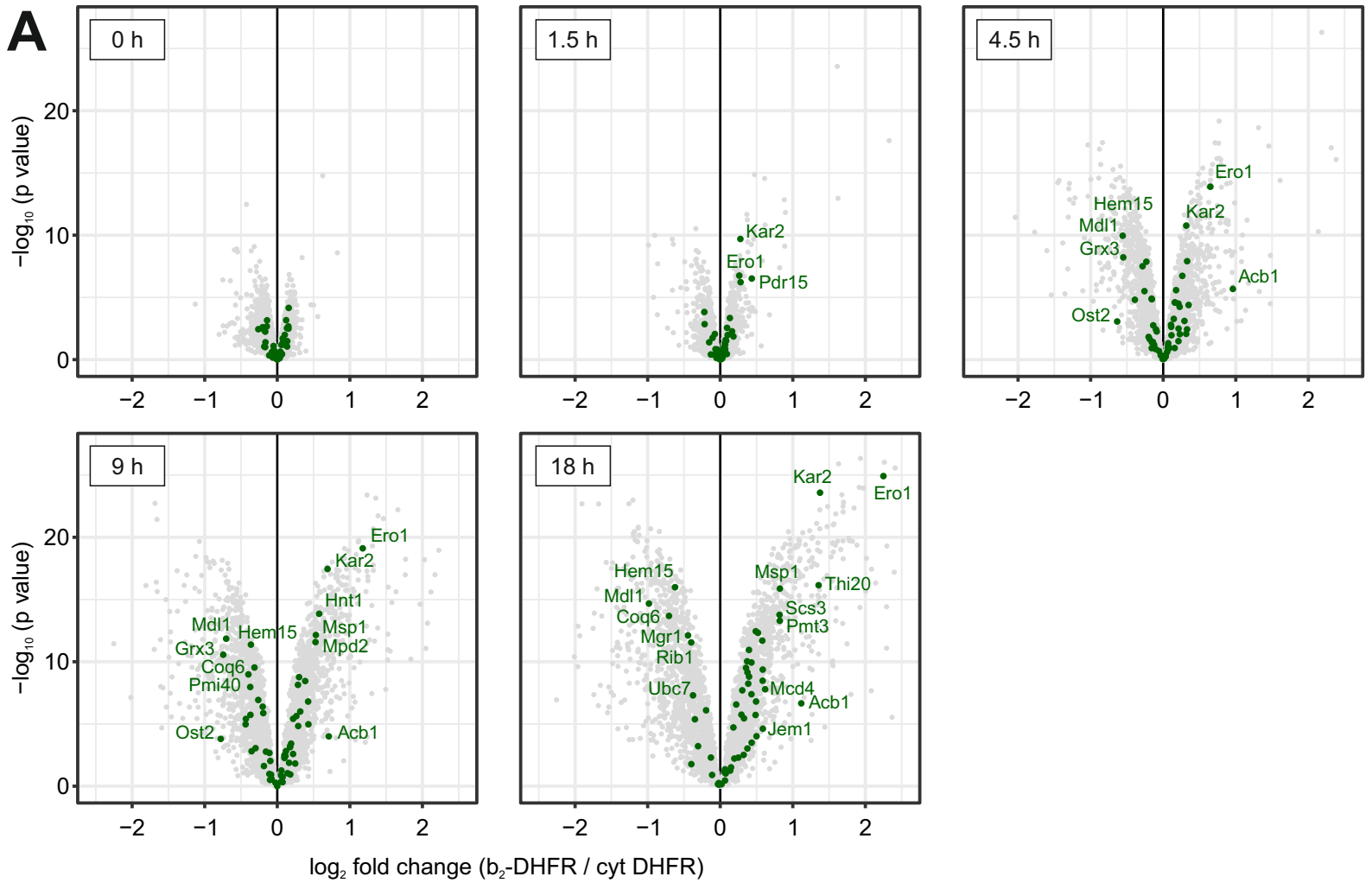
A
0 h
1.5 h
4.5 h
9 h
18 h
−log10 (p value)
log2 fold change (b2-DHFR / cyt DHFR)
Kar2
Ero1
Pdr15
Hem15
Mdl1
Grx3
Acb1
Ost2
Hnt1
Msp1
Mpd2
Coq6
Pmi40
Thi20
Scs3
Pmt3
Mgr1
Rib1
Ubc7
Mcd4
Jem1

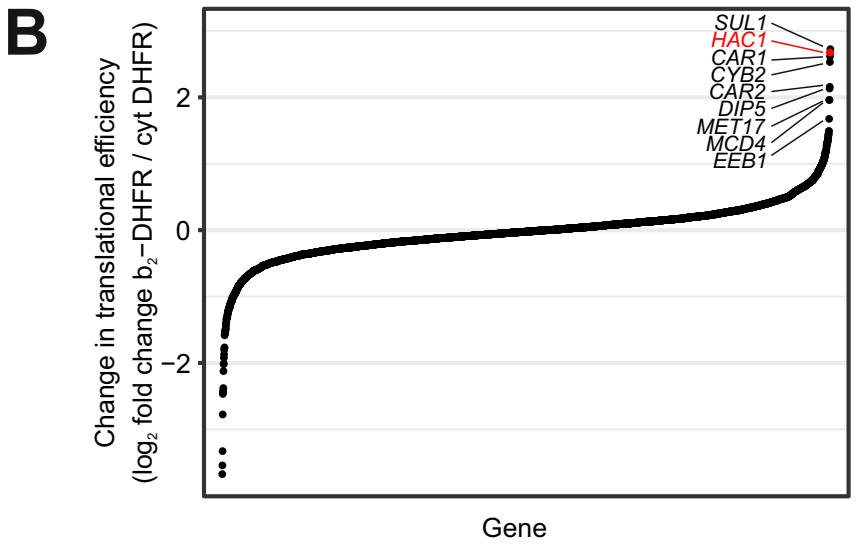
B
Change in translational efficiency
(log2 fold change b2−DHFR / cyt DHFR)
Gene
SUL1
HAC1
CAR1
CYB2
CAR2
DIP5
MET17
MCD4
EEB1

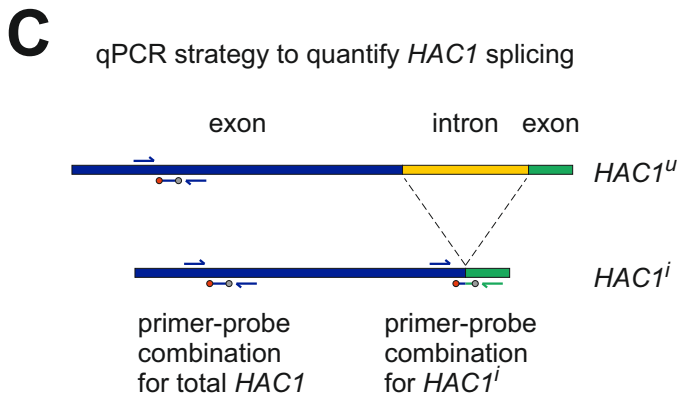
C
qPCR strategy to quantify HAC1 splicing
exon
intron
exon
HAC1u
HAC1i
primer-probe combination for total HAC1
primer-probe combination for HAC1i

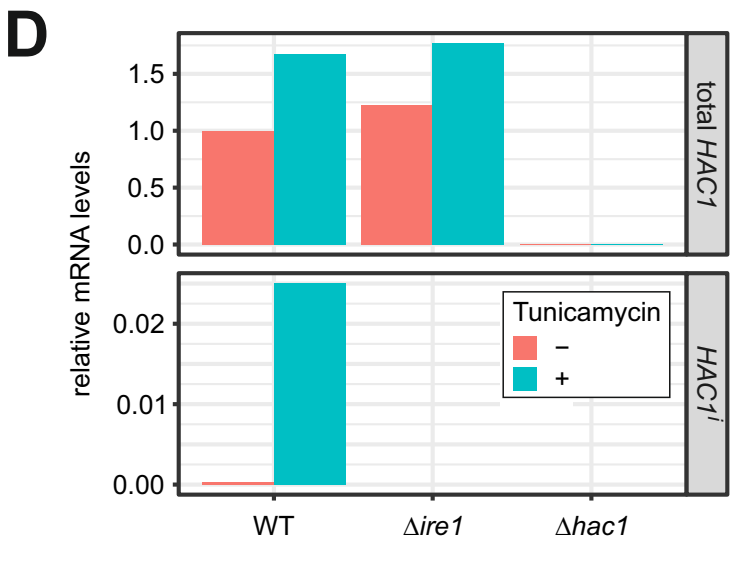
D
relative mRNA levels
total HAC1
HAC1i
Tunicamycin
−
+
WT
Δire1
Δhac1

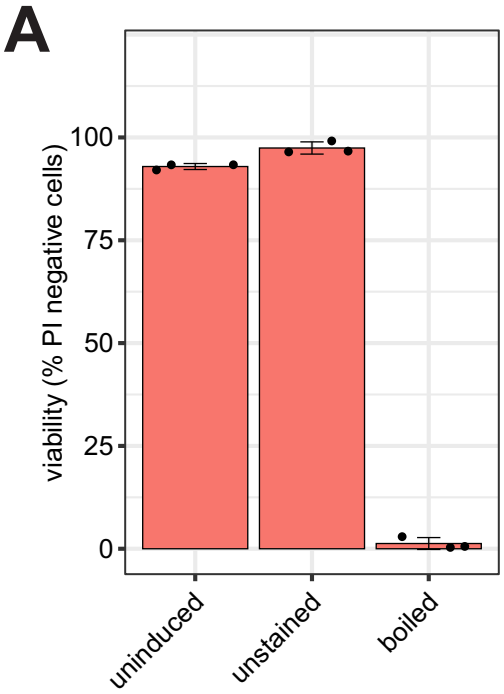
A
viability (% PI negative cells)
100
75
50
25
0
uninduced
unstained
boiled

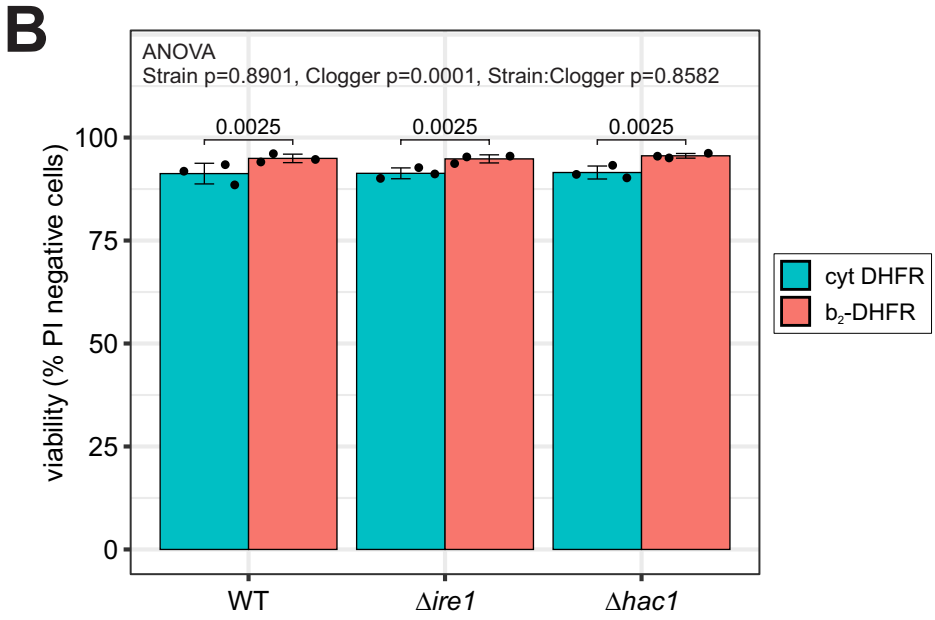
B
ANOVA
Strain p=0.8901, Clogger p=0.0001, Strain:Clogger p=0.8582
viability (% PI negative cells)
100
75
50
25
0
0.0025
0.0025
0.0025
WT
Δire1
Δhac1
cyt DHFR
b2-DHFR

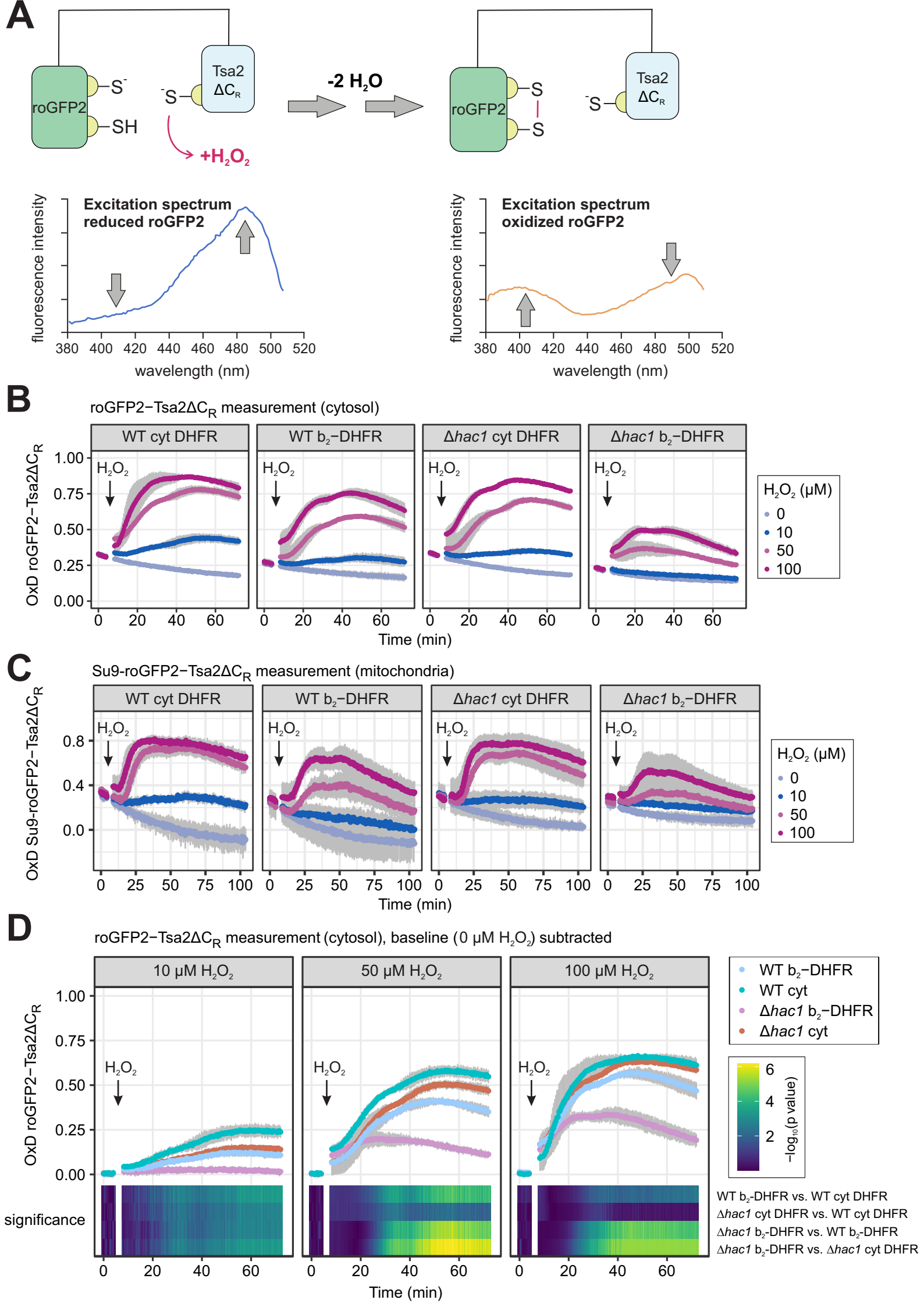
A
roGFP2
S⁻
SH
Tsa2 ΔC_R
⁻S
+H2O2
-2 H2O
roGFP2
S
S
⁻S
Tsa2 ΔC_R
fluorescence intensity
Excitation spectrum reduced roGFP2
380 400 420 440 460 480 500 520
wavelength (nm)
fluorescence intensity
Excitation spectrum oxidized roGFP2
380 400 420 440 460 480 500 520
wavelength (nm)
B
roGFP2−Tsa2ΔC_R measurement (cytosol)
WT cyt DHFR
WT b2−DHFR
Δhac1 cyt DHFR
Δhac1 b2−DHFR
H2O2
OxD roGFP2−Tsa2ΔC_R
1.00
0.75
0.50
0.25
0.00
0 20 40 60
Time (min)
H2O2 (μM)
0
10
50
100
C
Su9-roGFP2−Tsa2ΔC_R measurement (mitochondria)
WT cyt DHFR
WT b2−DHFR
Δhac1 cyt DHFR
Δhac1 b2−DHFR
H2O2
OxD Su9-roGFP2−Tsa2ΔC_R
0.8
0.4
0.0
0 25 50 75 100
Time (min)
H2O2 (μM)
0
10
50
100
D
roGFP2−Tsa2ΔC_R measurement (cytosol), baseline (0 μM H2O2) subtracted
10 μM H2O2
50 μM H2O2
100 μM H2O2
H2O2
OxD roGFP2−Tsa2ΔC_R
1.00
0.75
0.50
0.25
0.00
significance
0 20 40 60
Time (min)
WT b2−DHFR
WT cyt
Δhac1 b2−DHFR
Δhac1 cyt
6
4
2
−log10(p value)
WT b2-DHFR vs. WT cyt DHFR
Δhac1 cyt DHFR vs. WT cyt DHFR
Δhac1 b2-DHFR vs. WT b2-DHFR
Δhac1 b2-DHFR vs. Δhac1 cyt DHFR

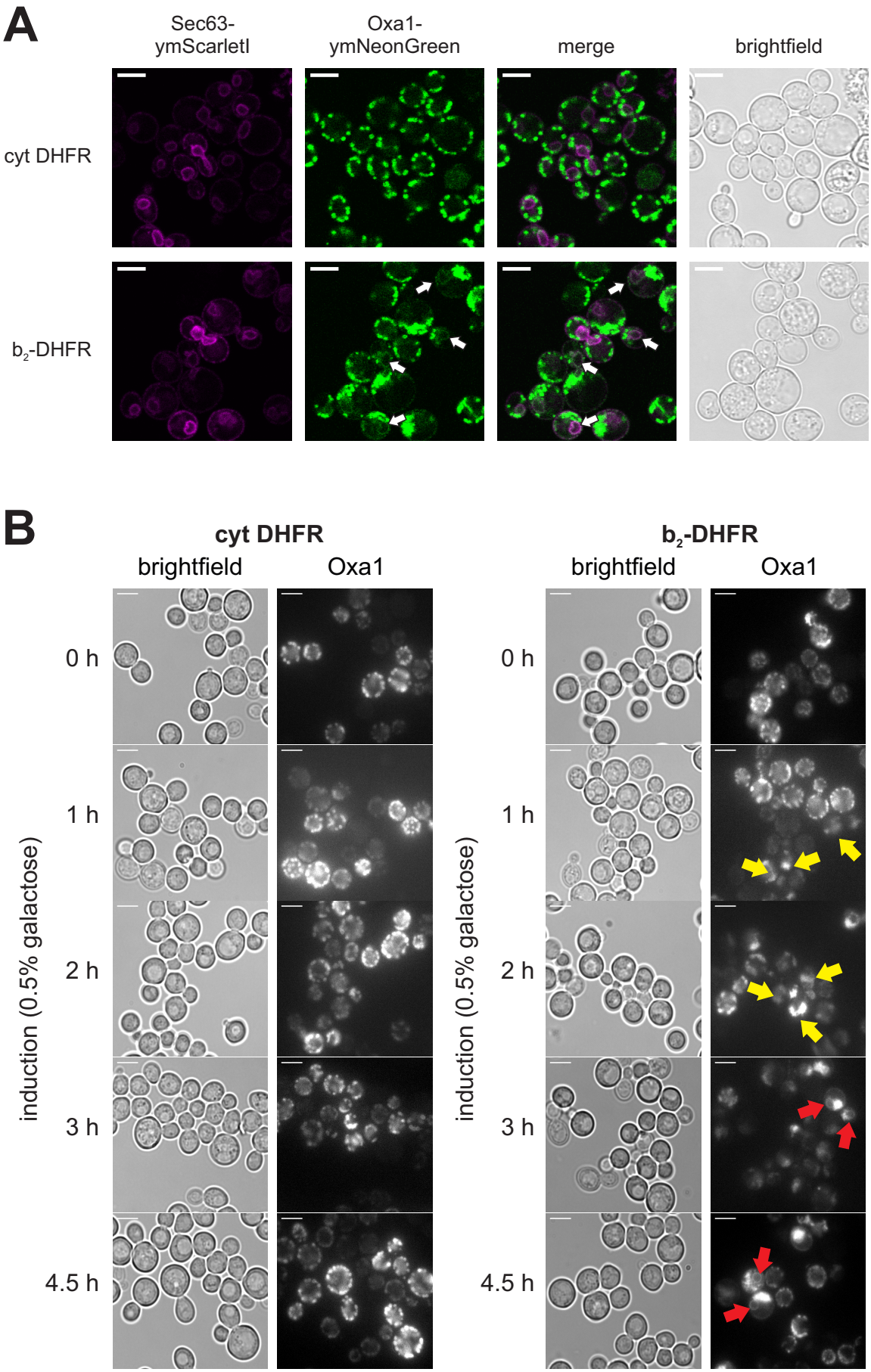
A
Sec63-ymScarletI
Oxa1-ymNeonGreen
merge
brightfield
cyt DHFR
b2-DHFR
B
cyt DHFR
b2-DHFR
brightfield
Oxa1
0 h
1 h
2 h
3 h
4.5 h
induction (0.5% galactose)
altered mitochondrial morphology
ring-shaped ER structure

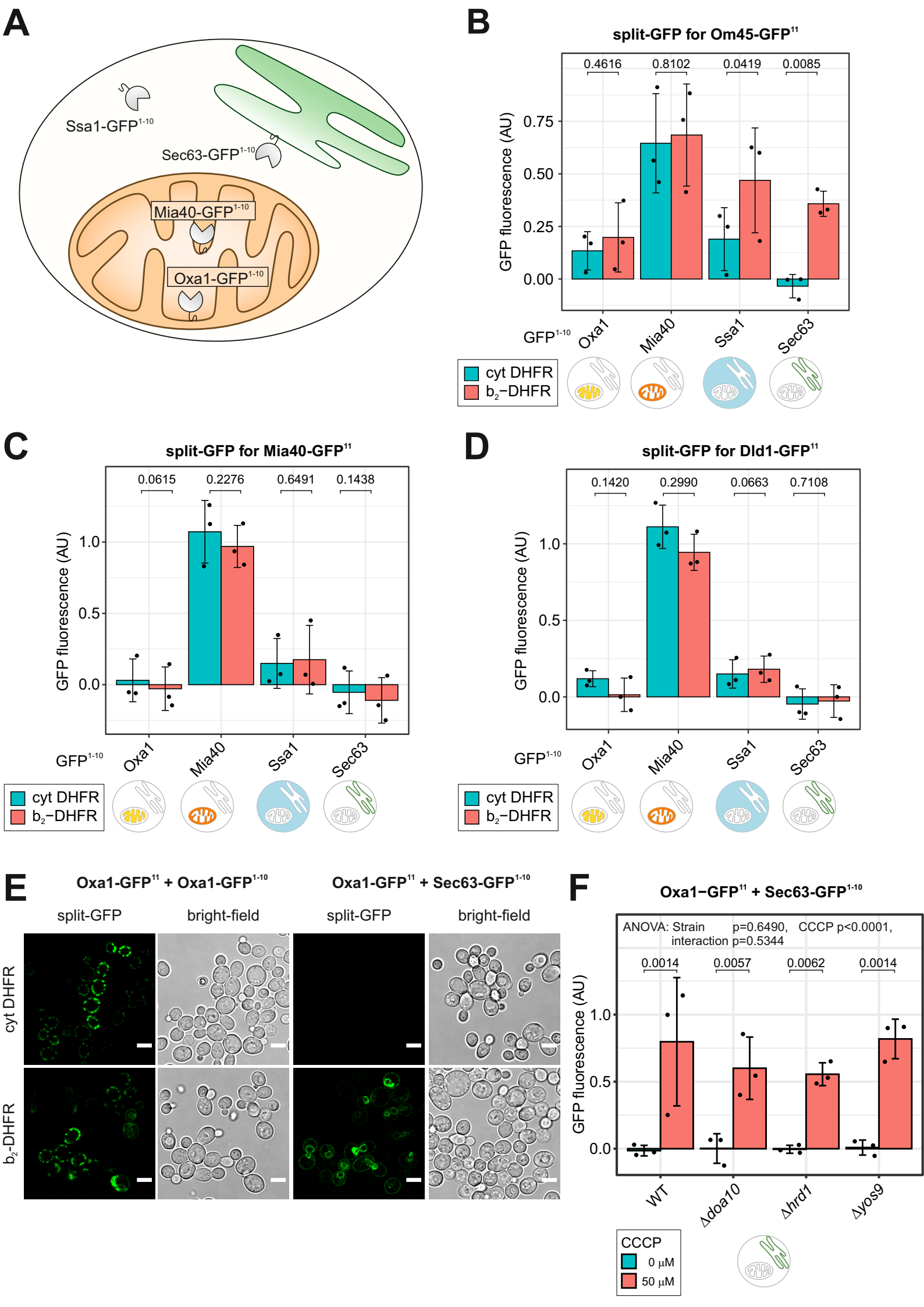
A
Ssa1-GFP1-10
Sec63-GFP1-10
Mia40-GFP1-10
Oxa1-GFP1-10
B
split-GFP for Om45-GFP11
0.4616
0.8102
0.0419
0.0085
GFP fluorescence (AU)
0.75
0.50
0.25
0.00
GFP1-10
Oxa1
Mia40
Ssa1
Sec63
cyt DHFR
b2−DHFR
C
split-GFP for Mia40-GFP11
0.0615
0.2276
0.6491
0.1438
GFP fluorescence (AU)
1.0
0.5
0.0
GFP1-10
Oxa1
Mia40
Ssa1
Sec63
cyt DHFR
b2−DHFR
D
split-GFP for Dld1-GFP11
0.1420
0.2990
0.0663
0.7108
GFP fluorescence (AU)
1.0
0.5
0.0
GFP1-10
Oxa1
Mia40
Ssa1
Sec63
cyt DHFR
b2−DHFR
E
Oxa1-GFP11 + Oxa1-GFP1-10
Oxa1-GFP11 + Sec63-GFP1-10
split-GFP
bright-field
split-GFP
bright-field
cyt DHFR
b2-DHFR
F
Oxa1−GFP11 + Sec63-GFP1-10
ANOVA: Strain p=0.6490, CCCP p<0.0001,
interaction p=0.5344
0.0014
0.0057
0.0062
0.0014
GFP fluorescence (AU)
1.0
0.5
0.0
WT
Δdoa10
Δhrd1
Δyos9
CCCP
0 μM
50 μM

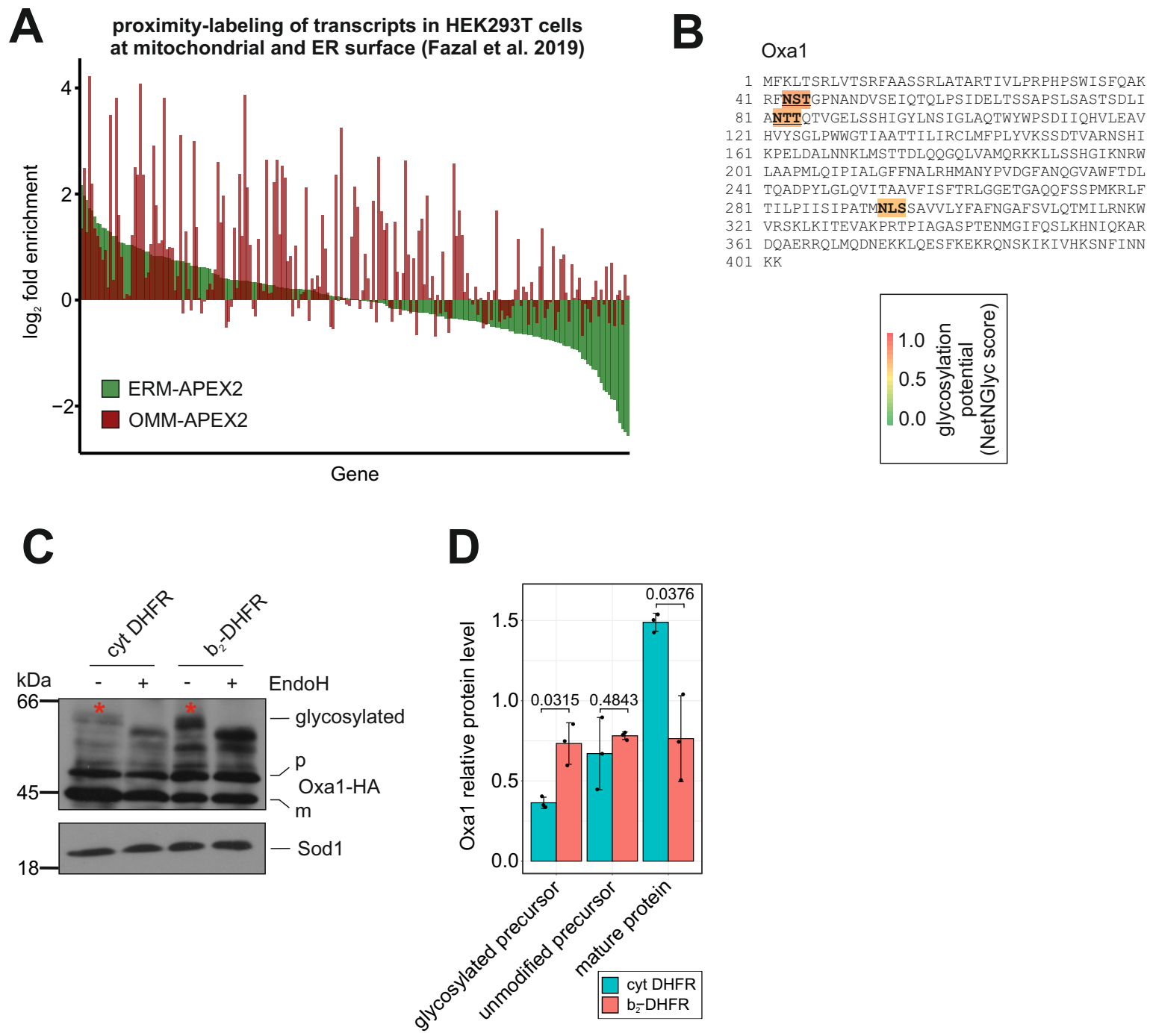
A
proximity-labeling of transcripts in HEK293T cells
at mitochondrial and ER surface (Fazal et al. 2019)
log2 fold enrichment
4
2
0
−2
ERM-APEX2
OMM-APEX2
Gene
B
Oxa1
1 MFKLTSRLVTSRFAASSRLATARTIVLPRPHPSWISFQAK
41 RFNSTGPNANDVSEIQTQLPSIDELTSSAPSLSASTSDLI
81 ANTTQTVGELSSHIGYLNSIGLAQTWYWPSDIIQHVLEAV
121 HVYSGLPWWGTIAATTILIRCLMFPLYVKSSDTVARNSHI
161 KPELDALNNKLMSTTDLQQGQLVAMQRKKLLSSHGIKNRW
201 LAAPMLQIPIALGFFNALRHMANYPVDGFANQGVAWFTDL
241 TQADPYLGLQVITAAVFISFTRLGGETGAQQFSSPMKRLF
281 TILPIISIPATMNLSSAVVLYFAFNGAFSVLQTMILRNKW
321 VRSKLKITEVAKPRTPIAGASPTENMGIFQSLKHNIQKAR
361 DQAERRQLMQDNEKKLQESFKEKRQNSKIKIVHKSNFINN
401 KK
1.0
0.5
0.0
glycosylation potential (NetNGlyc score)
C
cyt DHFR
b2-DHFR
kDa
- + - +
EndoH
66
45
18
glycosylated
p
Oxa1-HA
m
Sod1
D
Oxa1 relative protein level
1.5
1.0
0.5
0.0
0.0376
0.0315
0.4843
glycosylated precursor
unmodified precursor
mature protein
cyt DHFR
b2-DHFR

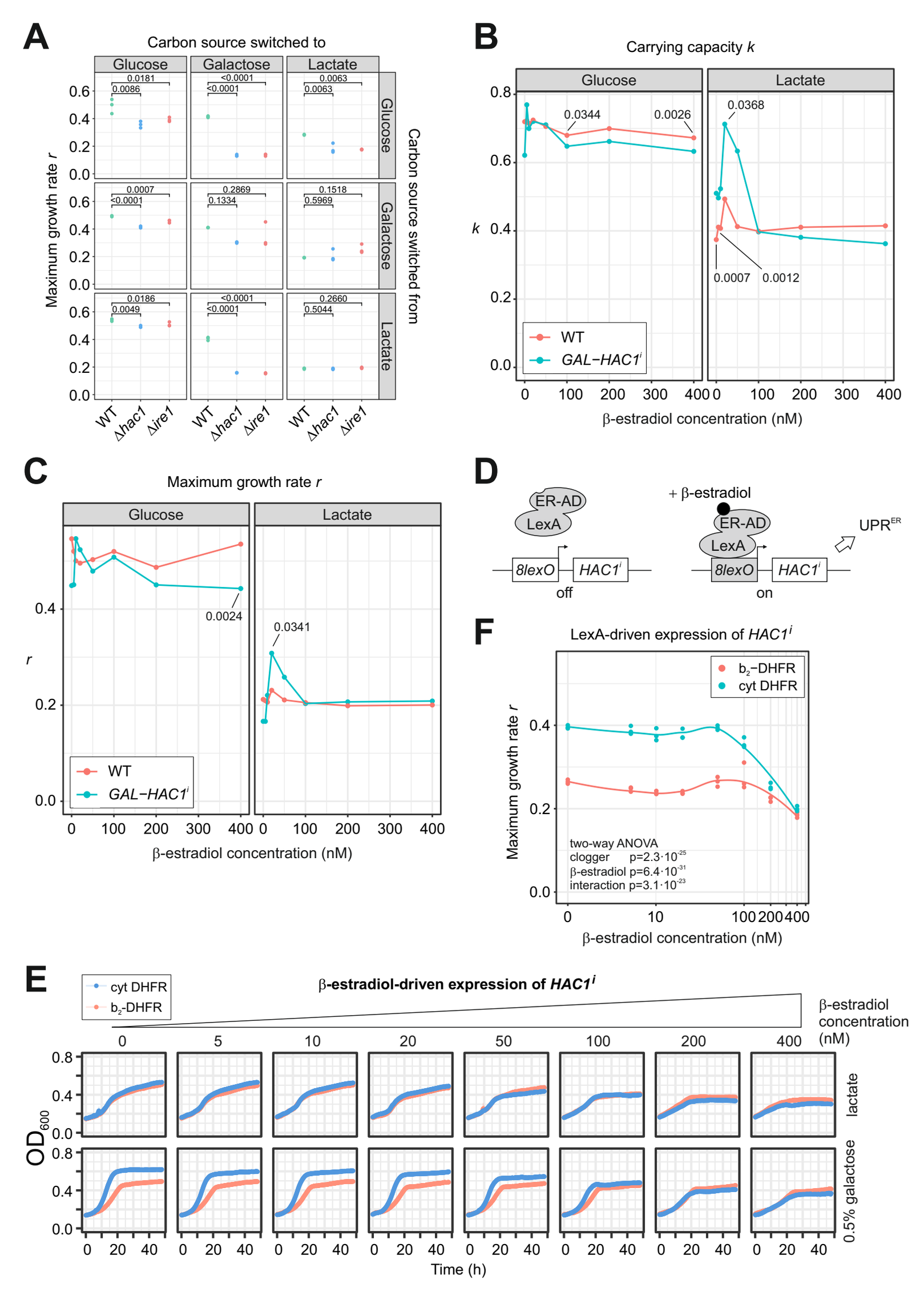
A
Carbon source switched to
Glucose
Galactose
Lactate
Carbon source switched from
Maximum growth rate r
0.0181
0.0086
<0.0001
<0.0001
0.0063
0.0063
0.0007
<0.0001
0.2869
0.1334
0.1518
0.5969
0.0186
0.0049
<0.0001
<0.0001
0.2660
0.5044
WT
Δhac1
Δire1
B
Carrying capacity k
k
0.0344
0.0026
0.0368
0.0007
0.0012
WT
GAL−HAC1i
β-estradiol concentration (nM)
C
Maximum growth rate r
r
0.0024
0.0341
D
ER-AD
LexA
8lexO
HAC1i
off
+ β-estradiol
on
UPRER
F
LexA-driven expression of HAC1i
b2−DHFR
cyt DHFR
Maximum growth rate r
two-way ANOVA
clogger p=2.3·10-25
β-estradiol p=6.4·10-31
interaction p=3.1·10-23
β-estradiol concentration (nM)
E
β-estradiol-driven expression of HAC1i
cyt DHFR
b2-DHFR
β-estradiol concentration (nM)
0
5
10
20
50
100
200
400
OD600
lactate
0.5% galactose
Time (h)

Figure 1B Original Data

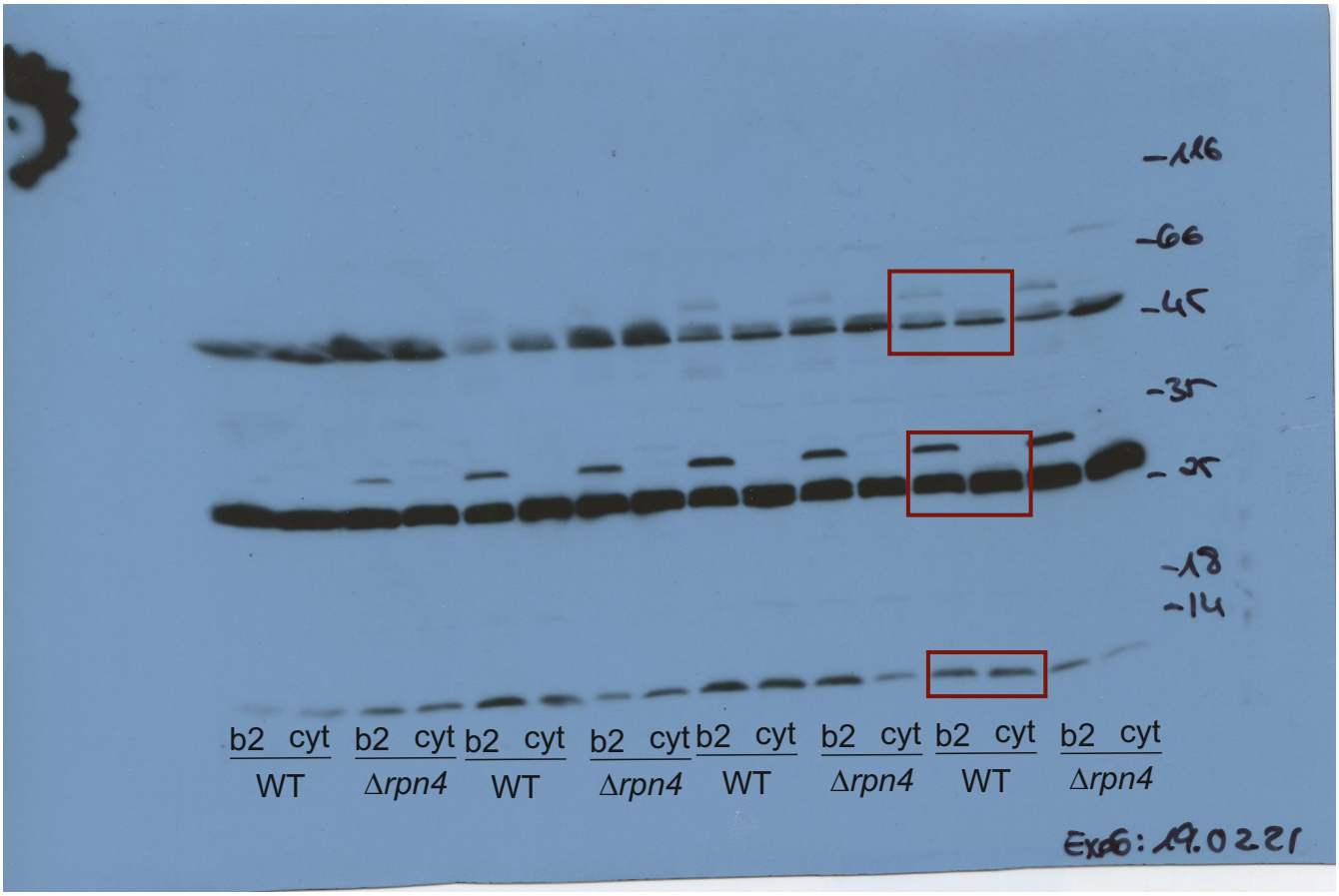

Supplementary Figure 7C Original Data

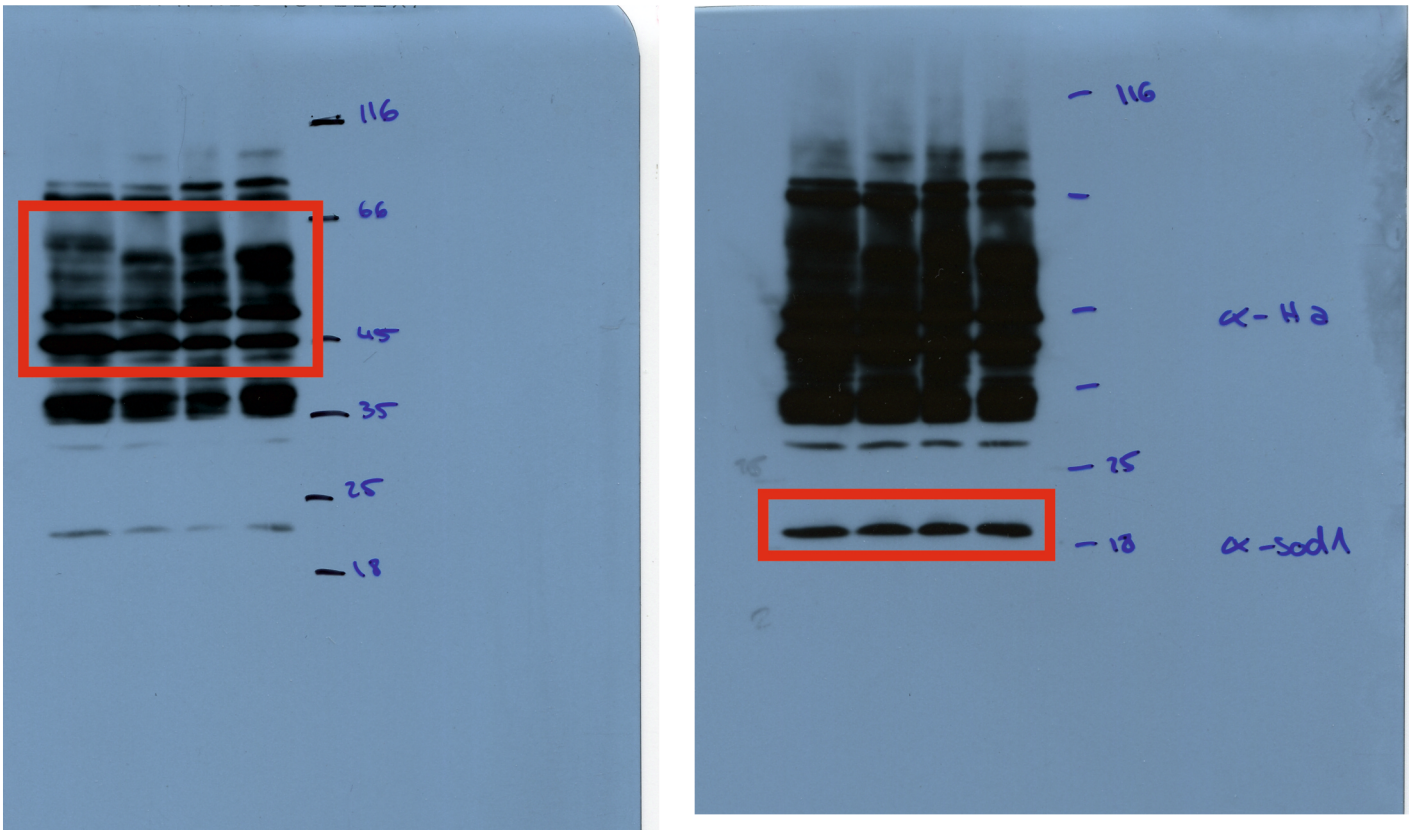

The films show two different exposures of the same Western Blot